PLANNING MALAYSIA:
Journal of the Malaysian Institute of Planners
VOLUME 21 ISSUE 2 (2023), Page 1 – 12

ANALYSIS OF FLASH FLOOD POTENTIAL INDEX (FFPI) AND SCENARIOS ASSESSMENT IN SHAH ALAM USING GIS APPROACH

Nurul A. Mohd Yassin[1], Nor Aizam Adnan[2], Eran S. S. Md Sadek[3]

[1,2,3]*Centre of Studies for Surveying Science and Geomatics,*
College of Built Environment,
UNIVERSITI TEKNOLOGI MARA, SHAH ALAM SELANGOR,
MALAYSIA

Abstract

Nowadays, there is an increase in the frequency of flash floods, which can have disastrous effects on both the economy and people's lives. In this study, the flash floods in Shah Alam are analysed using the Flash Flood Potential Index (FFPI) assessment method, which utilises four significant parameters, namely ground slope, land use, soil type, and NDVI, as outlined in the FFPI model that was first developed in 2003. The study reveals that the study area has a medium risk of flash floods, with an index value of five (5) to six (6). Flash flood risk is considered in all study scenarios, with a probability of over 50%. Scenario 2 produces the best results, with a 71% chance of Shah Alam being hit by a high-level flash flood and a 22% chance of being hit by a medium-level flash flood. Since the FFPI is a dimensionless index ranging from 1 to 10, and the percentage of FFPI in Shah Alam is 47.48% for the value of 5 (median index), it is concluded that Shah Alam is in the medium risk group for daily flash floods. The FFPI is a suitable index to be used in Malaysia for predicting urban flood risk. Additionally, it is recommended to incorporate the calculation of factors or parameters that contribute to flash floods using weighting and ranking, particularly related to the drainage system and precipitation.

Keywords: Flash Flood, Shah Alam, Flash Flood Potential Index, Geographic Information System, GIS, Remote Sensing

[3] Corresponding author

INTRODUCTION

Floods, haze, and drought are among the mild climate-related disasters commonly experienced in Malaysia, but floods are known to have severe socio economic repercussions on the nation. The effects and scenarios of climate change in Malaysia are significant, evident in changes in temperature, heavy rainfall, impacts on human health, changes in coastal areas, sea-level rise, effects on biodiversity, changes in land cover, availability of water resources, and crop productivity (Rahman, 2018). Flash floods are the most destructive natural disaster in Malaysia, particularly in urban areas, and have become increasingly evident to metropolitan populations, causing infrastructure damage, injuries, economic disruptions, and disruptions to daily routines (Abdul Malek et al., 2020).

In recent decades, Malaysia has been hit by various extreme weather and climatic events, such as La Niña and monsoons in Kuala Lumpur and Selangor in December 2011 (The Star, 2011). On December 27, 2021, Malaysia's floods resulted in the highest-ever unpredictability, with 48 fatalities reported (Bernama, 2021). Flash floods, which occur quickly, can cause severe economic and fatal damages, despite their rarity (Bhuiyan et al., 2021), with land factors and heavy rain as the major contributors (Muhamed Noordin et al., 2007). Recent flood monitoring efforts have heavily relied on remote sensing and GIS, focusing on delineating flood zones, creating flood hazard and risk maps for vulnerable locations. This integration of knowledge and technology has already been applied in other places, such as Ethiopia (Bishaw, 2012). In this study, GIS techniques and the Flash Flood Potential Index (FFPI) were employed to identify flash flood factors, understand flash flood locations, classify flash flood risk levels, and verify flash flood classifications using historical data and remote sensing images in Shah Alam.

DATA AND METHODS USED FOR FFPI

Data Collection for Flash Flood Potential Index (FFPI)

The data are both in vector and raster format. Table 1 shows the data collected for the classification of flash flood potential and meanwhile the data collected for the verification is from this source https://browser.creodias.eu.

Table 1: Data Collected and Used For FFPI

Datasets	DEM	Soil type	Landcover	Vegetation
Sources	Shuttle Radar Topography Mission (SRTM) [2015]	Digital Soil Map of the World (DSMW) [2007]	Land Use/Land Cover (LULC) [1/2/2021]	Landsat-8 [7/2/2021]

Source: United States Geological Survey (USGS), Food and Agriculture Organization (FAO) & ESRI

Data Preparation for FFPI

This study utilised four different parameters of data in accordance with the Flash Flood Potential Index (FFPI). These factors include slope, soil, land use/land cover (LULC), and vegetation index of NDVI, which were prepared and classified in accordance with FFPI requirements, as shown in Table 3. Slope is a crucial element as it controls runoff. Figure 1(a) displays the slope percentage of the study area, while Figure 1(b) shows the FFPI-reclassified slope. Figure 2(a) depicts the soil types in the study area, with Orthic Acrisols being clay-rich acidic soils with deep, loamy, dark brown soil and Dystric Histosols containing over 14% organic matter. Eutric Gleysols are water-saturated, non-salted soils. The reclassified soil map is displayed in Figure 2(b).

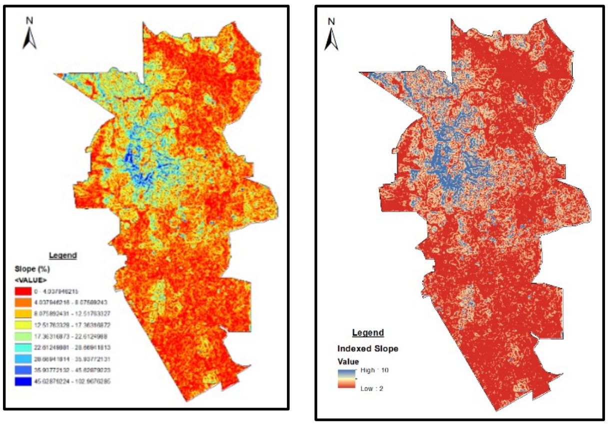

(a) (b)

Figure 1: Slope Factor of FFPI: (a) Slope Map, (b) Reclassified Slope Map
Source: Author's Output

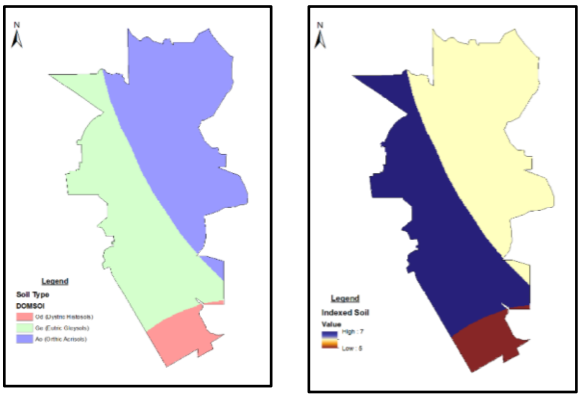

(a) (b)

Figure 2: Soil Factor of FFPI: (a) Soil Map, (b) Reclassified Soil Map
Source: Author's Output

The type of land use and land cover (LULC) for the study area is shown in Figure 3(a). In Shah Alam, the majority of the land is covered by built-up areas such as buildings, roads, and highways, which make the surface less permeable to water. Figure 3(b) shows the reclassification of LULC used in FFPI. The vegetation index of NDVI uses red and near-infrared wavelengths to enhance vegetation features and canopy structure through spectral imaging transformation. By using NDVI and satellite images, the extent of flooding can be estimated for various flood occurrences. Figure 4(a) shows the vegetation index of the study area, while Figure 4(b) displays the reclassified NDVI factor.

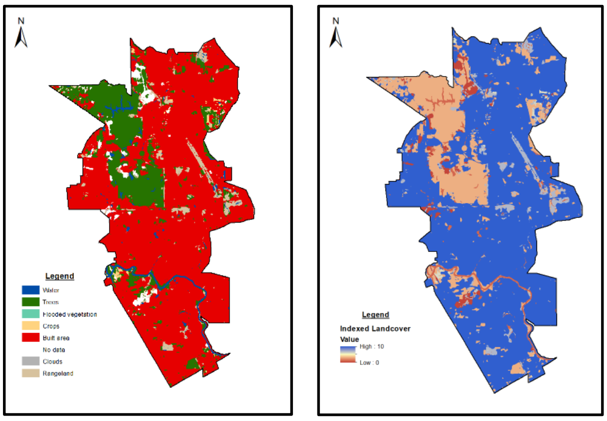

(a) (b)

Figure 3: Landcover Factor of FFPI: (a) Landcover Map, (b) Reclassified Landcover Map

Source: Author's Output

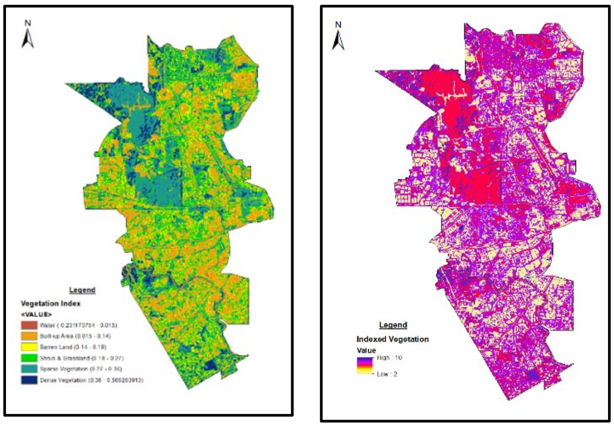

(a) (b)

Figure 4: Vegetation Factor of FFPI: (a) Vegetation Map, (b) Reclassified Vegetation Map

Source: Author's Output

Calculation of FFPI

In 2003, the FFPI was developed by the National Weather Service's Colorado Basin River Forecast Centre, which takes into account slope, vegetation cover/density, soil texture, and land use (Smith, 2003). The FFPI is generated by collecting raster datasets of these attributes across the region of interest and then using GIS technology to resample, reclassify, and combine the data. Figure 5 illustrates the steps involved in processing the data using the FFPI approach. The result is a numerical index that indicates a region's potential for flash flooding, which remains relatively static over time.

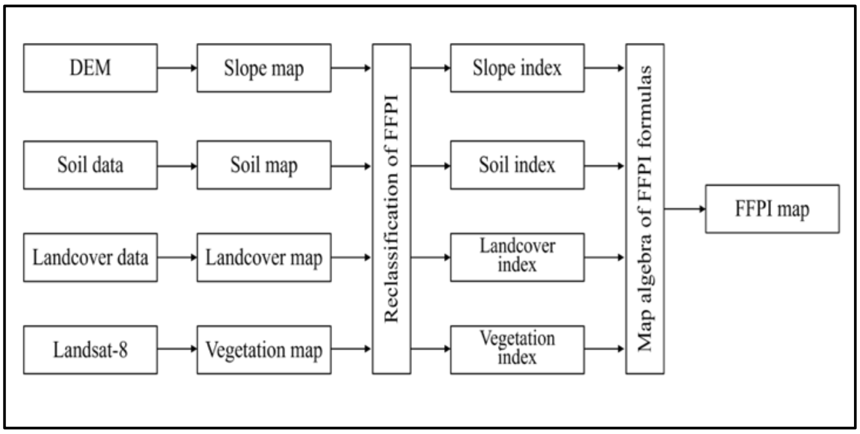

Figure 5: Methodology Flow Chart Using FFPI.
Source: Author's Illustration

A GIS can be utilised to classify, compare and assess the intrinsic flash flood potential of a particular drainage basin to provide quantitative information (Kruzdlo & Ceru, 2010). The hydrologic response attributes of each data layer were assigned a flash flood potential index ranging from 1-10. In the previous study, an equal interval classification was used (Arachchige & Perera, 2015). Each factor was given a score between 1 and 10 on the index, where a value of 1 indicates a low probability of flash floods, and a value of 10 indicates the highest probability. Table 2 displays the FFPI values assigned to each dataset based on its sensitivity to flash flooding.

Table 2: Assigned FFPI Values on Each Dataset Depending on The Susceptibility for Flash Flooding

FFPI value	Slope/DEM (%)	Land use	Vegetation cover (%)	Soil type
1	3 and below	Water	90 – 100	Water/Alluvial
2	6	Woody Wetlands, Herbaceous Wetland	80 – 89	Sand
3	9	Evergreen Forest	70 – 79	Sandy Loam

4	12	Mixed Forest	60 – 69	Silty Loam, Loamy sand
5	15	Deciduous Forest	50 – 59	Silt/Organic matter
6	18	Pasture Hay, Cultivated	40 – 49	Loam
7	21	Developed/open space, Barren Land	30 – 39	Sandy Clay Loam, Silty Clay Loam
8	24	Developed/low	20 – 29	Clay Loam, Sandy, Clay
9	27	Developed/medium	10 – 19	Clay
10	30 and above	Developed/heavy	0 – 9	Bed, Rock/Impervious

Source: (Smith, 2003), (Kruzdlo & Ceru, 2010), (Arachchige & Perera, 2015), (Brewster, 2004), (Smith, 2010), (Minea, 2013), (Zogg & Deitsch, 2013) & (Shawaqfah et al., 2020)

Smith (2003) introduced the factors or parameters of the FFPI which have since been utilised by numerous researchers, as presented in Table 3. An updated version of the FFPI assigned greater importance to slope than to vegetation cover, resulting in a higher likelihood of flash floods occurring in areas with steeper slopes (Brewster, 2009). The most significant change was that each component was given an equal weighting (Kruzdlo & Ceru, 2010). Another modification was that more emphasis was placed on a slope as well as land cover/use (Ceru, 2012).

The generation of the FFPI map involves the use of raster map algebra in the Spatial Analyst tool within ArcGIS. Different formulas are employed for four scenarios, as depicted in Table 3, to determine the flash flood potential using the FFPI approach. Upon computation of the FFPI, a second reclassification step is conducted to determine the severity of the risk level associated with the possibility of flash flooding.

Table 3: Equations Used for FFPI Scenarios

Scenario	Equation used	Factors used	Notes
1	$\frac{(1.5M + L + S + V)}{4.5}$	Slope, land cover, soil type, vegetation cover	(Smith, 2003)
2	$\frac{(1.5(M) + L + S + 0.5(V))}{4}$	Slope, land cover, soil type, vegetation cover	(Brewster, 2009)
3	$\frac{(M + L + S + V)}{4}$	Slope, land cover, soil type, vegetation cover	(Kruzdlo & Ceru, 2010)
4	$\frac{(2(M) + 2(L) + S + V)}{6}$	Slope, land cover, soil type, vegetation cover	(Ceru, 2012)

Source: (Shawaqfah et al., 2020)

Verification of Results Using Historical Flood Data

After the FFPI classification is completed, verification is carried out using historical data from remote sensing imagery that correspond with flash flood events. To observe flood situations from space, the active satellite data system, Spaceborne Synthetic Aperture Radar (SAR), is widely used as it can penetrate cloud coverage, operate during day and night, and function effectively during adverse weather conditions like heavy rainfall. The software provided by Sentinel, SNAP software, is utilised to process this satellite imagery. Another method employed for the verification of the FFPI classification is Kernel Density, which is used to locate the hotspot area based on the obtained historical flood data. Historical flood information for Shah Alam was obtained from the Selangor Department of Irrigation and Drainage in the form of vector data presented as points.

RESULTS AND DISCUSSIONS

Four Scenarios FFPI in Shah Alam and Percentage Area of FFPI Value

Figure 6(a) to 6(d) show the result from the first, second, third and fourth equations of FFPI used respectively as described in Table 4 and known as Scenario 1, Scenario 2, Scenario 3, and Scenario 4. The figures range from the value 2 to 9 of the index in Table 3 where the lowest potential is in the dark brown colour and the highest potential is in the dark green colour. These figures show that most of the study area is classed as having a medium potential value for flash floods, with values ranging from 5 to 6.

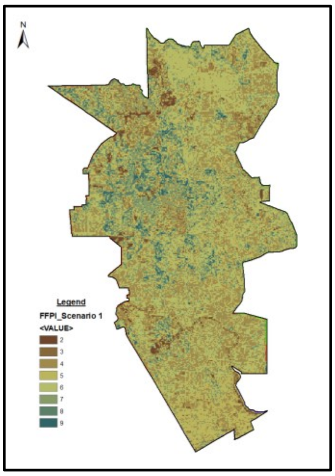

(a)

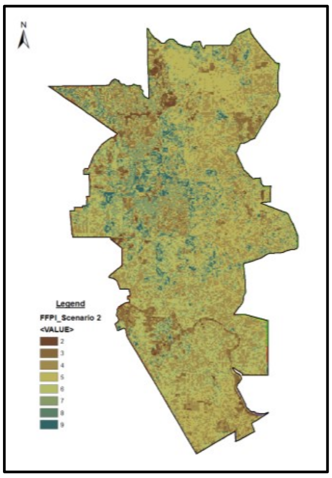

(b)

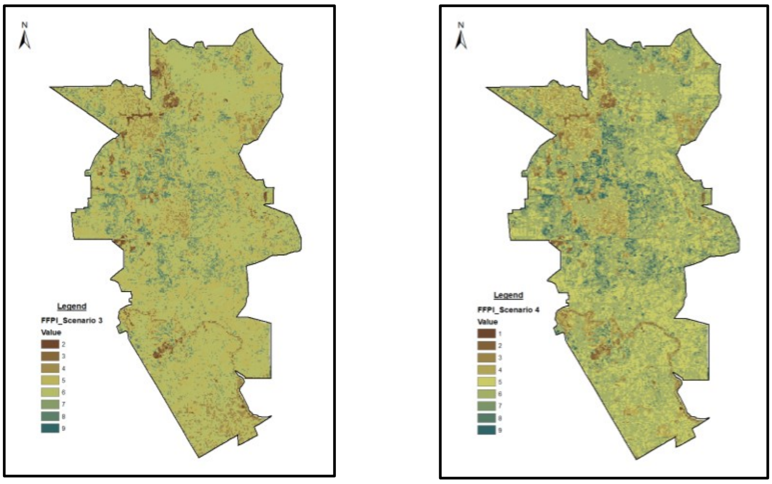

(c) (d)

Figure 6: FFPI of Shah Alam: (a) Scenario 1, (b) Scenario 2, (c) Scenario 3, (d) Scenario 4.

Source: Author's Output

The area of the FFPI value in each scenario is calculated in the form of percentage as shown in Table 4. The outcomes from each scenario indicated that the potential index of flash flood is in the middle of the range spanning from the least potential to the most potential. On the other hand, Scenario 3, and Scenario 4 have values that range from five to seven as the highest possible within the scenario itself. Both hypothetical situations cover more than 40% of the research field when the FFPI is set to six. It appears that both outcomes place the study area at a medium risk of experiencing a flash flood. Areas at medium risk include Setia Alam, Sections 2, 19, 23, and Bukit Kemuning, which are overlayed on a base map.

Table 4: Percentage of Area in FFPI Scenarios

FFPI	Percentage of area belong to different FFPI values (%)			
	Scenario 1	Scenario 2	Scenario 3	Scenario 4
1	0.00	0.00	0.00	0.01
2	1.03	0.78	0.78	1.50
3	1.53	3.85	1.38	4.65
4	27.51	9.91	7.15	7.65
5	23.93	47.48	34.28	25.91
6	36.51	28.29	40.28	43.70
7	7.63	7.09	13.62	12.42
8	1.85	2.13	2.48	2.90
9	0.01	0.47	0.01	1.25
10	0.00	0.00	0.00	0.00

Source: Author's Calculation

Comparison of FFPI Risk Level with Hotspot Area of Historical Data of Flash Flood Occurrence

The analysis of historical data is conducted to identify the area where flash floods frequently occur during the years of interest. The hotspot region of flash floods in Shah Alam is depicted in Figure 7(a). By comparing it to Figure 7(b), it can be observed that the hotspot area of flash flood occurrence lies within the high-risk region susceptible to flash flooding. However, the area with the highest potential for flash flooding, i.e., the extreme-risk area, does not overlap with the hotspot area of flash flood occurrence. This area has experienced infrequent flooding events, as per the past data.

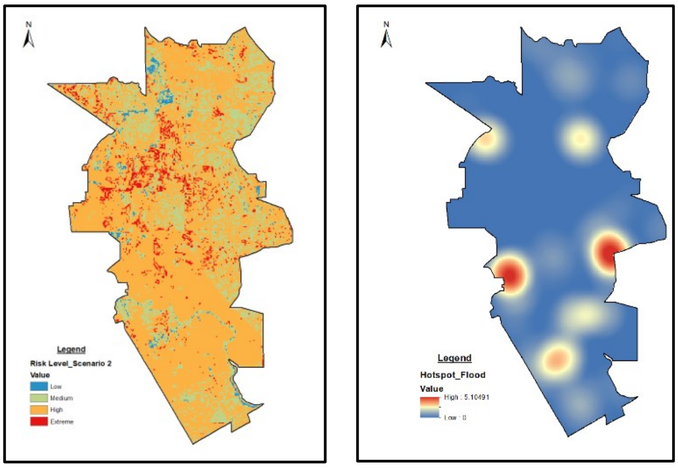

(a) (b)

Figure 7: Comparison of Outcomes: (a) FFPI Risk Level, (b) Hotspot Area of Historical Data

Source: Author's Output

Comparison of Historical Data of Flash Flood Occurrence with FFPI

The reclassification of FFPI into four risk levels, namely low, medium, high, and extreme, overlaid with historical flash flood data is shown in Figure 8(a), while the flood extends map area results obtained from the SAR image of Sentinel-1 GRD data is shown in Figure 8(b). The flood occurred in the red area within the yellow circle in Figure 8(b), and upon comparison with the area depicted within the yellow circle in Figure 8(a), it can be inferred that the flood happened in the high-risk area of flash flooding in accordance with its potential. The radar image indicates that the region that was potentially extremely vulnerable to flash flooding did not appear to have been impacted by the said disaster.

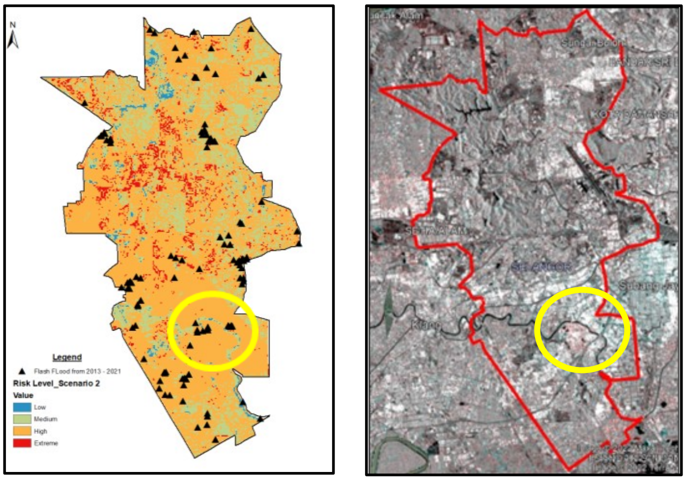

(a) (b)

Figure 8: Comparison of Outcomes: (a) Historical Data, (b) Flood Extent
Source: Author's Output

Discussion on Method Used for Study Area

As mentioned earlier, it was noted that in the area that was highly susceptible to flash flooding according to FFPI, flash floods occurred rarely, as expected from the obtained results. This suggests that the outcomes obtained in this section may not accurately reflect the actual situation, where the area is expected to experience extreme flash flooding. To address this, an enhanced and more comprehensive version of FFPI, known as FFPI Weights-Of-Evidence (FFPI WofE), was developed in 2022. It incorporates additional factors such as elevation, aspect, profile curvature, depth of fragmentation, Stream Power Index (SPI), Topographic Wetness Index (TWI), Topographic Position Index (TPI), precipitation, lithology, and Hydrologic Soil Group (HSG). A new WofE equation, which uses deterministic weighted average spatial analysis, was applied, and the resulting output was divided into five FFPI vulnerability classes (Kocsis et al., 2022).

Most previous studies focused on areas within river basins and catchments where natural flash floods occur. This is the primary reason why the results of this study differ, as the study area is located in an urban region where floods are caused mostly by human activities, known as urban flash floods. Man-made structures like drainage systems play a significant role in urban flash floods. The lack of important factors in this study might have affected the results. Precipitation is also a crucial factor to consider since urban flash floods are usually caused by prolonged and heavy rainfall in urban areas, resulting in an increase in stormwater levels.

CONCLUSION

FFPI is a tool used by researchers and policymakers to identify areas that are susceptible to flash floods and can be used to provide information on flood risk reduction aspects for Development Proposal Report (DPR) (Afida et al. 2016). In Malaysia, FFPI has not yet been implemented in any region of the country. This study incorporates four original factors, including slope, soil, vegetation, and landcover, which have been previously used in research conducted around the world. The findings indicate that Scenario 2 yielded the best results and suggest that Shah Alam has a 71% chance of experiencing a high-level flash flood and a 22% chance of experiencing a medium-level flash flood. The FFPI is a model that provides an index ranging from 1 to 10, and given that Shah Alam's FFPI is at 47.5% for an index value of 5, which is the median, it can be classified as being at medium risk for flash floods. While the results are not entirely satisfactory, they do demonstrate the potential of Shah Alam given that the primary factors have been considered. By incorporating an additional factor, such as the one discussed, more reasonable results may be obtained.

REFERENCES

Abdul Malek, N., Zayid, S., Ahmad, Z., Ya'acob, S., & Abu Bakar, N. (2020). Data Understanding for Flash Flood Prediction in Urban Areas. *Journal of Environmental Treatment Techniques, 8*(2), 770-778.

Afida, I., Idrus, S., & Hashim, H. S. (2016). Information Quality For Flood Risk Reduction In Site Planning: Town Planners' Perception. *Planning Malaysia: Journal of the Malaysian Institute of Planners*, 14, 39-54

Arachchige. R. & Perera D. J., (2015). Mapping Flash Flood Potential Using GIS and the Flash Flood Potential Index (FFPI) In the Turtle River and Forest River Watersheds In North Dakota. Retrieved from https://commons.und.edu/theses

Bernama. (2021, December 30). *Major floods mark the end of 2021.* Retrieved from The Malaysian Reserve: https://themalaysianreserve.com/2021/12/30/major-floods-mark-the-end-of-2021/

Bhuiyan, T. R., Er, A. C., Muhamad, N., & Pereira, J. J. (2021). The socioeconomic impact of climate-related hazards: flash flood impact assessment in Kuala Lumpur, Malaysia. *Natural Hazards, 109*(20), 1509-1538.

Bishaw, K. (2012). Application of GIS and Remote Sensing Techniques for Flood Hazard and Risk Assessment: The Case of Dugeda Bora Woreda of Oromiya Regional State, Ethiopia. *Conference on the Human Dimensions of Global Environmental Change* (pp. 1-17). Berlin: Institutional Repository of the Freie Universität Berlin.

Brewster, J. (2004). The Flash Flood Potential Index for Central New York and Northeast Pennsylvania. Binghamton

Brewster, J. (2009), Development of the Flash Flood Potential Index. A Microsoft PowerPoint presentation retrieved from: http://www.erh.noaa.gov/bgm/research/ERFFW/presentations/june_02_2010/Brewster_Jim_Development_of_FFPI.ppt. 2009

Ceru, J. (2012). The Flash Flood Potential Index for Pennsylvania. Retrieved from *https://proceedings.esri.com/library/userconf/feduc12/papers/user/joeceru.pdf*

Kocsis, I., Bilașco, Ștefan, Irimuș, I. A., Dohotar, V., Rusu, R., & Roșca, S. (2022). Flash Flood Vulnerability Mapping Based on FFPI Using GIS Spatial Analysis Case Study: Valea Rea Catchment Area, Romania. *Sensors, 22*(9), 1–21.

Kruzdlo, R., & Ceru, J. (2010). National Oceanic and Atmospheric Administration. Retrieved from Flash Flood Potential Index for WFO Mount Holly/Philadelphia. Retrieved from http://bgmresearch.eas.cornell.edu/research/ERFFW/posters/kruzdlo_FlashFloodPotentialIndexforMountHollyHSA.pdf

Minea, G. (2013). Assessment of the Flash Flood Potential of Bâsca River Catchment (Romania) Based on Physiographic Factors. *Central European Journal of Geosciences, 5*(3), 344-353.

Muhamed Noordin, N., Abdullah, A., & Azraei Shahbudin, M. (2007). Multicriteria Analysis of Flood Causes in Kuala Lumpur. *Planning Malaysia*: *Journal of the Malaysian Institute of Planners, 5,* 17-42.

Rahman, H. A. (2018). Climate Change Scenarios in Malaysia: *Engaging the Public. International Journal of Malay-Nusantara Studies, 1*(2), 55-77.

Shawaqfah, M., AlMomani, F., & Khatatbeh, A. (2020). Mapping Flash Flood Potential and Risk Level Using GIS Techniques and the Flash Flood Potential Index (FFPI) in Amman Zarqa Basin of Jordan. *Jordanian Journal of Engineering and Chemical Industries, 3*(3), 81-90.

Smith, G. (2003) *Flash flood potential: determining the hydrologic response of FFMP basins to heavy rain by analysing their physiographic characteristics.* A white paper available from the NWS Colorado Basin River Forecast Centre. Retrieved from *http://www.cbrfc. noaa.gov/papers/ffp_wpap.pdf*

Smith, G. E. (2010). Development of a flash Flood Potential Index Using Physiographic Datasets within a Geographic Information System. Retrieved from *https://collections.lib.utah.edu/ark:/87278/s6ft91hc*

The Star. (2011, December 6). 'Terrible twins' La Nina and monsoon to hit KL and Selangor. Retrieved from The Star: https://www.thestar.com.my/news/nation/2011/12/06/terrible-twins-la-nina-and-monsoon-to-hit-kl-and-selangor

Zogg, J., & Deitsch K. (2013). The flash flood potential index at WFO Des Moines, Iowa. Retrieved from *http://www.crh.noaa. gov/Image/dmx/hydro/FFPI/FFPI_WriteUp.pdf*

Received: 2nd May 2023. Accepted: 7th June 2023

